NASA TECHNICAL NOTE

NASA TN D-4990

NASA TN D-4990

EFFECTS OF STRUCTURAL DAMPING ON FLUTTER OF STRESSED PANELS

by Charles P. Shore

Langley Research Center
Langley Station, Hampton, Va.

NATIONAL AERONAUTICS AND SPACE ADMINISTRATION • WASHINGTON, D. C. • JANUARY 1969

EFFECTS OF STRUCTURAL DAMPING ON FLUTTER OF STRESSED PANELS

By Charles P. Shore

Langley Research Center
Langley Station, Hampton, Va.

NATIONAL AERONAUTICS AND SPACE ADMINISTRATION

For sale by the Clearinghouse for Federal Scientific and Technical Information
Springfield, Virginia 22151 – CFSTI price $3.00

EFFECTS OF STRUCTURAL DAMPING ON FLUTTER OF STRESSED PANELS*

By Charles P. Shore
Langley Research Center

SUMMARY

The flutter of stressed orthotropic panels with edge rotational restraint is investigated theoretically. A modal solution which utilizes two-dimensional quasi-steady aerodynamic theory and includes both structural and aerodynamic damping is presented. The investigation was conducted in an attempt to explain the existing discrepancies between theoretical and experimental results for stressed panels, in particular for panels stressed near buckling, the most critical flutter condition. Structural damping is represented in the present analysis in a manner consistent with the representation for a Kelvin-Voigt viscoelastic body. Numerical results are presented to indicate that such a representation of structural damping eliminates the physically untenable results that have been obtained for certain values of the input parameters in previous analyses. Additionally, representation of structural damping in this manner results in a reasonable correlation between theory and experiment over the entire range of stress from zero to buckling.

INTRODUCTION

Recent studies of panel flutter (refs. 1 and 2) have shown that inclusion of the effects of edge rotational restraint can improve the agreement between theoretical and experimental flutter results for stressed isotropic panels. However, many instances remain where large discrepancies exist between theory and experiment for such panels. Theory which neglects damping predicts zero dynamic pressure required for flutter whenever the midplane load has caused two panel vibration frequencies to be equal. This condition occurs for panels with a length-width ratio greater than 1 for many combinations of stress ratio and edge rotational restraint. On the other hand, experimental flutter boundaries display none of the anomalous behavior associated with coincidence of the theoretical

*A part of the information presented herein was included in a thesis entitled "Flutter of Stressed Panels Including Effects of Edge Rotational Restraint and Damping" submitted in partial fulfillment of the requirements for the degree of Master of Science in Engineering Mechanics, Virginia Polytechnic Institute, Blacksburg, Virginia, March 1967.

frequencies. In fact, most experimental data show that the minimum value of dynamic pressure for flutter occurs at or near the transition point, which is the intersection of the panel prebuckled boundary and the postbuckled boundary. For examples of this behavior, see references 2 and 3.

Inclusion of aerodynamic and structural damping in the flutter theory can remove zero-dynamic-pressure flutter points. (See refs. 4 and 5.) However, the effects of aerodynamic and viscous structural damping (employed in refs. 6 and 7) decrease with increasing compressive stress and vanish at the transition point (ref. 5). Reference 8 points out that viscous-type damping is not a realistic approximation of the damping characteristics of structural materials and should, therefore, be applied with caution. Another formulation for structural damping frequently utilized in aeroelastic studies is the frequency independent linear hysteretic form. Although the mechanisms responsible for damping in structures are usually nonlinear, for small amounts of damping the linear model often provides a good approximation (ref. 9). In references 5 and 10 to 14 a linear hysteretic structural damping coefficient is, in effect, used to modify both the bending and membrane loading terms of the flutter equation. However, the effect of structural damping when employed in this manner also decreases with an increase in compressive stress and vanishes at the transition point (refs. 4 and 5). Hence, this approach predicts the same anomalous behavior as the theory that ignores damping. However, vibration equations derived on the basis of viscoelastic theory utilizing stress-strain relations for a Kelvin-Voigt body (ref. 15) indicate that linear hysteretic structural damping should modify only those terms of the equations associated with bending. Such a procedure is believed to lead to the correct form of the equations and is the basis for the flutter analysis developed in the present paper. However, in order to compare present results with results from previous investigations, two separate damping coefficients are introduced, one associated with the membrane or inplane forces and the other associated with panel bending. A solution for the flutter of orthotropic, flat, rectangular panels with arbitrary edge rotational restraint is obtained by application of the Galerkin procedure. It is assumed that the lateral loading is given by two-dimensional quasi-steady approximate aerodynamic theory.

Results from the analysis are presented to indicate that the use of the two-dimensional quasi-steady aerodynamic theory yields satisfactory results for problems in which the effects of aerodynamic damping are important. Additional results are presented to indicate that inclusion of structural damping in flutter theory is more realistically accomplished by use of linear hysteretic structural damping associated with panel bending only. Such a procedure removes all physically untenable effects that otherwise occur and renders the value of the flutter parameter at the transition point relatively insensitive to variations in length-width ratio, stress ratio, and edge rotational restraint. Finally, a comparison of results from the present analysis with existing experimental results is

presented to verify the improved correlation between theory and experiment for flutter of stressed panels over the entire stress range from zero to buckling.

SYMBOLS

A_{rs} Fourier series coefficient

a panel length

B_1, B_2, B_3, B_4 coefficients defined by equations (17)

b panel width

C_0, C_1, C_2 constants defined by equations (A2)

c free-stream speed of sound

D_x panel bending stiffness in x-direction

D_y panel bending stiffness in y-direction

D_{xy} panel twisting stiffness

D_1, D_{12}, D_2 panel stiffness coefficients defined by equations (9)

E Young's modulus

F_r streamwise deflection function

G_s cross-stream deflection function

g structural damping coefficient

g_A aerodynamic damping coefficient, $\frac{\rho c}{\gamma \omega_r}$

g_B bending structural damping coefficient

g_M membrane structural damping coefficient

$i = \sqrt{-1}$

$(I_1)_{mr}, (I_2)_{mr}, (I_3)_{mr}$ coefficients defined by equations (A3), (A4), and (A5)

$(J_1)_{mm}, (J_2)_{mm}, (J_2)_{mr}, (J_3)_{mm}$ coefficients defined by equations (A12) to (A15)

$(K_1)_{mm}, (K_2)_{mm}, (K_2)_{mr}, (K_3)_{mm}$ coefficients defined by equations (A16) to (A19)

k_x nondimensional stress coefficient in x-direction, $\frac{N_x b^2}{\pi^2 D_1}$

$k_{x,cr}$ buckling load with no airflow

$k_{x,T}$ buckling load with airflow

k_y nondimensional stress coefficient in y-direction, $\frac{N_y b^2}{\pi^2 D_1}$

k_1, k_2 constants

L_{mr} coefficient defined by equation (A6)

$\bar{L}_{mr}$ coefficient defined by equation (A20)

$\hat{L}_{mr}$ coefficient defined by equation (A21)

$l(x,y,t)$ aerodynamic loading term

M Mach number

N_x inplane loading in x-direction, positive in compression

N_y inplane loading in y-direction, positive in compression

p modulus of a complex number defined by equation (22)

q free-stream dynamic pressure

q_x rotational restraint coefficient on $x = \pm\frac{a}{2}$ boundary, $\frac{a\theta_x}{D_1}$

q_y rotational restraint coefficient on $y = \pm\frac{b}{2}$ boundary, $\frac{b\theta_y}{D_2}$

t	time
U	free-stream air velocity
w	lateral deflection of panel
x,y,z	Cartesian coordinates of panel
α	complex frequency coefficient, $\varphi + i\omega$
β	compressibility factor, $\sqrt{M^2 - 1}$
γ	panel mass per unit area
δ_j	constant dependent on degree of rotational restraint
ϵ	strain
ϵ_0	maximum strain amplitude
θ_x,θ_y	spring constant of rotational spring supporting panel on boundary $x = \pm\frac{a}{2}$ and boundary $y = \pm\frac{b}{2}$, respectively
λ	dynamic-pressure parameter
λ_T	dynamic-pressure parameter at transition point
μ_x,μ_y	Poisson's ratio in x-direction and y-direction, respectively
ρ	free-stream air density
σ	stress
φ	real part of complex frequency exponential coefficient
ψ	complex eigenvalue (see eq. 18)
ψ_R	real part of complex eigenvalue
ψ_I	imaginary part of complex eigenvalue

ω circular frequency

ω_r reference frequency

Subscripts:

m,r number of half-waves in streamwise direction

s number of half-waves in cross-stream direction

ANALYSIS

The flat, rectangular, orthotropic panel configuration under consideration is shown in figure 1. The panel which is of length a and width b is exposed to supersonic flow over one surface and is subjected to uniform inplane force intensities N_x and N_y which are positive in compression. The panel is supported such that the lateral deflection on all edges is zero. Additionally, the panel edges are assumed to be elastically restrained from rotations by restoring moments which are of equal strength on opposite edges and are proportional to the edge angle of rotation.

Differential Equation and Boundary Conditions

The small-deflection equilibrium equation for motion of an orthotropic panel in the presence of inplane tensile or compressive loads and supersonic flow may be written in the following form (ref. 16):

$$\frac{D_x}{1 - \mu_x\mu_y}\frac{\partial^4 w}{\partial x^4} + 2\left(D_{xy} + \frac{\mu_y D_x}{1 - \mu_x\mu_y}\right)\frac{\partial^4 w}{\partial x^2 \partial y^2} + \frac{D_y}{1 - \mu_x\mu_y}\frac{\partial^4 w}{\partial y^4}$$

$$+ N_x\frac{\partial^2 w}{\partial x^2} + N_y\frac{\partial^2 w}{\partial y^2} + \gamma\frac{\partial^2 w}{\partial t^2} = l(x,y,t) \tag{1}$$

The panel bending stiffnesses in the x- and y-directions are denoted by D_x and D_y, respectively; D_{xy} is the panel twisting stiffness, and γ is the panel mass per unit area. The lateral loading induced by the supersonic flow is assumed to be given by two-dimensional quasi-steady aerodynamic theory so that (ref. 17)

$$l(x,y,t) = \frac{-2q}{\beta}\frac{\partial w}{\partial x} - \rho c\frac{\partial w}{\partial t} \tag{2}$$

where $q = \frac{1}{2}\rho U^2$ is the free-stream dynamic pressure and $\beta = \sqrt{M^2 - 1}$ is the

compressibility factor. The first term on the right-hand side of equation (2) corresponds to a static loading and the second term is a viscous loading corresponding to the aerodynamic damping. Reference 5 has shown that for $M > 1.6$ and $\frac{a}{b}$ from 0 to 10, the use of two-dimensional static aerodynamic theory (aerodynamic damping neglected) yields flutter results in good agreement with those predicted by more exact aerodynamic theory.

For finite rotational restraint and nondeflecting supports the boundary conditions (ref. 16) are as follows:

$$\left.\begin{aligned} \frac{D_x}{1 - \mu_x\mu_y}\frac{\partial^2 w}{\partial x^2} - \theta_x\frac{\partial w}{\partial x} = 0 \quad \text{and} \quad w = 0 \quad \text{at} \quad x = -\frac{a}{2} \\ \frac{D_x}{1 - \mu_x\mu_y}\frac{\partial^2 w}{\partial x^2} + \theta_x\frac{\partial w}{\partial x} = 0 \quad \text{and} \quad w = 0 \quad \text{at} \quad x = +\frac{a}{2} \end{aligned}\right\} \tag{3a}$$

$$\left.\begin{aligned} \frac{D_y}{1 - \mu_x\mu_y}\frac{\partial^2 w}{\partial y^2} - \theta_y\frac{\partial w}{\partial y} = 0 \quad \text{and} \quad w = 0 \quad \text{at} \quad y = -\frac{b}{2} \\ \frac{D_y}{1 - \mu_x\mu_y}\frac{\partial^2 w}{\partial y^2} + \theta_y\frac{\partial w}{\partial y} = 0 \quad \text{and} \quad w = 0 \quad \text{at} \quad y = +\frac{b}{2} \end{aligned}\right\} \tag{3b}$$

where θ_x and θ_y are the spring constants of the rotational springs on the boundaries $x = \pm\frac{a}{2}$ and $y = \pm\frac{b}{2}$, respectively.

The frequency-independent, linear, hysteretic formulation of structural damping is employed in the present analysis. Such a formulation may be derived for a one-dimensional case as follows. Assume that the material behaves as that for a Kelvin-Voigt viscoelastic body. For such a material the stress σ is a function of strain rate $\frac{\partial \epsilon}{\partial t}$ as well as of strain ϵ; thus,

$$\sigma = k_1\epsilon + k_2\frac{\partial \epsilon}{\partial t} \tag{4}$$

where k_1 represents the elastic modulus E and k_2 is a coefficient of viscosity; both k_1 and k_2 are positive real quantities.

For simple harmonic motion the strain may be written

$$\epsilon = \epsilon_0 e^{i\omega t} \tag{5}$$

where ϵ_0 is the maximum strain amplitude and ω is real.

The stress now becomes

$$\sigma = k_1\left(1 + i\omega \frac{k_2}{k_1}\right)\epsilon_0 e^{i\omega t} \tag{6}$$

where the term $i\omega \frac{k_2}{k_1}$ represents a stress 90^o out of phase with the strain. For frequency-independent, linear, hysteretic structural damping, $\frac{\omega k_2}{k_1}$ is replaced by a structural damping coefficient g which is independent of the magnitude of the frequency ω. The stress may now be written

$$\sigma = E(1 + ig)\epsilon_0 e^{i\omega t} \tag{7}$$

Thus, inclusion of this type of structural damping can be accomplished in dynamic analyses by using $(1 + ig)$ to modify all terms which contain the elastic modulus E. This procedure is most nearly correct for simple harmonic motion. Therefore, although this procedure may not be strictly valid for all regions of the solution to the present problem, it should yield good results at the point of sustained simple harmonic motion which is assumed to be the point of incipient flutter for the panel. With this procedure, only the terms in equation (1) involving panel bending will be modified by a structural damping coefficient. In reference 15 plate vibration equations utilizing stress-strain relations similar to equation (4) also indicate that only those terms of the equations associated with bending should be modified by a structural damping coefficient. However, in the present analysis a structural damping coefficient associated with membrane force terms is also retained so that the present results can be compared with those of previous investigations. The damping is introduced by multiplying the bending and membrane force terms in equation (1) by $\left(1 + ig_B\right)$ and $\left(1 + ig_M\right)$, respectively, where g_B and g_M are the bending and membrane structural damping coefficients. Such a procedure is equivalent to assuming complex bending stiffnesses and for $g_M \neq 0$, complex stress resultants.

Solution

Following the introduction of the generalized aerodynamic loading and the structural damping and dividing by $\frac{\pi^4 D_x}{1 - \mu_x\mu_y}$, equation (1) becomes

$$\left(1 + ig_B\right)\left(\frac{1}{\pi^4}\frac{\partial^4 w}{\partial x^4} + \frac{2}{\pi^4}\frac{D_{12}}{D_1}\frac{\partial^4 w}{\partial x^2 \partial y^2} + \frac{1}{\pi^4}\frac{D_2}{D_1}\frac{\partial^4 w}{\partial y^4}\right) + \left(1 + ig_M\right)\left(\frac{k_x}{\pi^2 b^2}\frac{\partial^2 w}{\partial x^2} + \frac{k_y}{\pi^2 b^2}\frac{\partial^2 w}{\partial y^2}\right)$$

$$+ \frac{1}{\omega_r{}^2 a^4}\frac{\partial^2 w}{\partial t^2} + \frac{g_A}{\omega_r a^4}\frac{\partial w}{\partial t} + \frac{\lambda}{\pi^4 a^3}\frac{\partial w}{\partial x} = 0 \tag{8}$$

where

$$D_1 = \frac{D_x}{1 - \mu_x\mu_y} \tag{9a}$$

$$D_{12} = D_{xy} + \frac{\mu_y D_x}{1 - \mu_x\mu_y} \tag{9b}$$

$$D_2 = \frac{D_y}{1 - \mu_x\mu_y} \tag{9c}$$

$$k_x = \frac{N_x b^2}{\pi^2 D_1} \tag{10a}$$

$$k_y = \frac{N_y b^2}{\pi^2 D_1} \tag{10b}$$

$$\omega_r{}^2 = \frac{\pi^4 D_1}{\gamma a^4} \tag{11}$$

$$g_A = \frac{\rho c}{\gamma \omega_r} \tag{12}$$

$$\lambda = \frac{2qa^3}{\beta D_1} \tag{13}$$

A solution to equation (8) for sustained motion of the panel may be obtained by application of the Galerkin technique. The lateral deflection is a function of the spatial coordinates x and y and time t and may be expressed in the form

$$w(x,y,t) = \sum_r \sum_s A_{rs} F_r\left(\frac{x}{a}\right) G_s\left(\frac{y}{b}\right) e^{\alpha t} \tag{14}$$

where α is of the form

$$\alpha = \varphi + i\omega \tag{15}$$

The deflection functions $F_r\left(\frac{x}{a}\right)$ and $G_s\left(\frac{y}{b}\right)$ are taken to be the zero-stress vibration-mode shapes for supported uniform beams with equal elastic end rotational restraints and hence satisfy all the boundary conditions (eqs. (3a) and (3b)). On the basis of past experience for a clamped panel (ref. 3), use of the beam vibration modes should yield excellent results.

Hedgepeth (ref. 18) has shown that for simple supports there is no stiffness coupling between cross-stream modes. In reference 19 it was indicated that such a coupling was insignificant for a fully clamped panel; therefore, coupling between cross-stream modes is assumed to be small for elastic restraints and is neglected herein. The two-dimensional aerodynamic theory precludes any aerodynamic coupling of orthogonal cross-stream modes. Thus, a one-term expansion in the cross-stream direction corresponding to the lowest beam vibration mode is used to determine the panel dynamic stability criterion. Substituting the assumed deflection (eq. (14)) into equation (8), multiplying by $F_m\left(\frac{x}{a}\right)G_1\left(\frac{y}{b}\right)$, integrating over the area, and noting that for a nontrivial solution to equation (8) the determinant of the coefficients of A_{r1} must equal zero yields the following stability criterion:

r \ m	1	2	3	4	
1	$\left(1+ig_B\right)\left[\left(\frac{1}{\pi^4}\right)\left(\frac{J_1}{J_3}\right)_{11}+B_1\left(\frac{J_2}{J_3}\right)_{11}+B_2\right]+\left(1+ig_M\right)\left[B_3\left(\frac{J_2}{J_3}\right)_{11}+B_4\right]+\psi$	$\frac{\lambda}{\pi^4}\frac{\bar{L}_{12}}{(J_3)_{11}}$	$\left[\left(1+ig_B\right)B_1+\left(1+ig_M\right)B_3\right]\frac{(J_2)_{13}}{(J_3)_{11}}$	$\frac{\lambda}{\pi^4}\frac{\bar{L}_{14}}{(J_3)_{11}}$	...
2	$\frac{\lambda}{\pi^4}\frac{\hat{L}_{21}}{(K_3)_{22}}$	$\left(1+ig_B\right)\left[\left(\frac{1}{\pi^4}\right)\left(\frac{K_1}{K_3}\right)_{22}+B_1\left(\frac{K_2}{K_3}\right)_{22}+B_2\right]+\left(1+ig_M\right)\left[B_3\left(\frac{K_2}{K_3}\right)_{22}+B_4\right]+\psi$	$\frac{\lambda}{\pi^4}\frac{\hat{L}_{23}}{(K_3)_{22}}$	$\left[\left(1+ig_B\right)B_1+\left(1+ig_M\right)B_3\right]\frac{(K_2)_{24}}{(K_3)_{22}}$	...
3	$\left[\left(1+ig_B\right)B_1+\left(1+ig_M\right)B_3\right]\frac{(J_2)_{31}}{(J_3)_{33}}$	$\frac{\lambda}{\pi^4}\frac{\bar{L}_{32}}{(J_3)_{33}}$	$\left(1+ig_B\right)\left[\left(\frac{1}{\pi^4}\right)\left(\frac{J_1}{J_3}\right)_{33}+B_1\left(\frac{J_2}{J_3}\right)_{33}+B_2\right]+\left(1+ig_M\right)\left[B_3\left(\frac{J_2}{J_3}\right)_{33}+B_4\right]+\psi$	$\frac{\lambda}{\pi^4}\frac{\bar{L}_{34}}{(J_3)_{33}}$	...
4	$\frac{\lambda}{\pi^4}\frac{\hat{L}_{41}}{(K_3)_{44}}$	$\left[\left(1+ig_B\right)B_1+\left(1+ig_M\right)B_3\right]\frac{(K_2)_{42}}{(K_3)_{44}}$	$\frac{\lambda}{\pi^4}\frac{\hat{L}_{43}}{(K_3)_{44}}$	$\left(1+ig_B\right)\left[\left(\frac{1}{\pi^4}\right)\left(\frac{K_1}{K_3}\right)_{44}+B_1\left(\frac{K_2}{K_3}\right)_{44}+B_2\right]+\left(1+ig_M\right)\left[B_3\left(\frac{K_2}{K_3}\right)_{44}+B_4\right]+\psi$	...
	⋮	⋮	⋮	⋮	

$= 0$ (16)

In the determinant of the coefficients of A_{r1}, the coefficients $(J_i)_{mr}$, $(K_i)_{mr}$, $\bar{L}_{mr}$, and $\hat{L}_{mr}$ represent integral expressions involving the streamwise deflection function and the constants C_0, C_1, and C_2 represent integral expressions involving the cross-stream deflection function. Details of the procedure and the integral expressions are given in the appendix. The coefficients B_1 to B_4 are given as

$$\left.\begin{aligned} B_1 &= \frac{2D_{12}}{\pi^2 D_1}\left(\frac{a}{b}\right)^2 \frac{C_1}{\pi^2 C_0} \\ B_2 &= \frac{D_2}{D_1}\left(\frac{a}{b}\right)^4 \frac{C_2}{\pi^4 C_0} \\ B_3 &= \frac{k_x}{\pi^2}\left(\frac{a}{b}\right)^2 \\ B_4 &= k_y\left(\frac{a}{b}\right)^4 \frac{C_1}{\pi^2 C_0} \end{aligned}\right\} \tag{17}$$

and

$$\psi = \psi_R + i\psi_I = \frac{\alpha^2}{\omega_r^2} + \frac{g_A}{\omega_r}\alpha \tag{18}$$

The expressions for B_1 and B_2 contain the panel geometric and stiffness parameters and the expressions for B_3 and B_4 contain the midplane loading terms k_x and k_y. The coefficients B_1, B_2, and B_4 are also functions of the cross-stream boundary conditions. (See the appendix.) The term ψ in equation (16) assumes the role of a complex eigenvalue which must be examined to determine the stability of the panel and includes both the panel frequencies and the aerodynamic damping coefficient.

The panel behavior is characterized by the variation of $\varphi + i\omega$ with an increase in aerodynamic load λ. Instability of the panel occurs when φ becomes positive and, hence, the condition when $\varphi = 0$ is taken to be the critical condition. This condition corresponds to sustained simple harmonic motion and represents incipient flutter for the panel. The relations necessary to determine φ and ω may be obtained by solving for α from equation (18), as follows:

$$\frac{\alpha}{\omega_r} = -\frac{g_A}{2} \pm \frac{1}{2}\sqrt{g_A^2 + 4(\psi_R + i\psi_I)} \tag{19}$$

Equation (19) yields two roots for α and, thus, two sets of $(\varphi + i\omega)$. The roots for ω occur as $\pm$ the same absolute quantity; however, examination of equations (6) and (7)

reveals that introduction of positive structural damping in the flutter equation implies that the algebraic sign of the damping coefficient g and ω be the same. Thus, for a positive damping coefficient g the solution is valid only for the root of α corresponding to positive values of ω. For certain panel conditions if both roots for α are considered, a false instability ($\varphi > 0$) is found to occur over a wide range of λ including $\lambda = 0$, a completely unrealistic result. The anomalies encountered in considering the negative root for ω have been noted by other authors in references 20 and 21.

Substituting equation (15) for α into equation (19), equating the real and imaginary parts, and selecting the root corresponding to positive ω yields

$$\frac{\varphi}{\omega_r} = -\frac{g_A}{2} + \frac{\psi_I}{2}\sqrt{\frac{p + g_A^2 + 4\psi_R}{2\psi_I^2}} \tag{20}$$

and

$$\frac{\omega}{\omega_r} = \frac{1}{2}\sqrt{\frac{p - g_A^2 - 4\psi_R}{2}} \tag{21}$$

where

$$p = \sqrt{\left(g_A^2 + 4\psi_R\right)^2 + \left(4\psi_I\right)^2} \tag{22}$$

Equations (20) and (21) govern both the dynamic and static stability of the panel. Zero values of the term under the radical in equation (21) yield zero values of the frequency which indicate zero stiffness and hence loss of static stability for the panel. Since $\varphi = 0$ is sought as the critical condition for dynamic instability, equation (20) is used to determine the relation between g_A and the real and imaginary parts of the eigenvalue ψ at flutter. The aerodynamic damping coefficient g_A is defined as a positive quantity; therefore, only positive values of ψ_I in equation (20) can lead to dynamic instability. The relation between g_A and the real and imaginary parts of the eigenvalue ψ thus obtained is

$$g_A = \frac{\psi_I}{\sqrt{-\psi_R}} \tag{23}$$

As both the aerodynamic damping and the structural damping approach zero, the use of equation (23) leads to values of λ which approach the values required for coalescence of the two lowest natural frequencies. In the presence of damping, flutter occurs at a value of λ corresponding to the value required to cause φ to become positive. For specific flow conditions and panel material, the aerodynamic damping coefficient may be expressed as a function of λ by combining equations (11) to (13) and is given by

$$g_A = \frac{1}{\pi^2}\left(\frac{\rho\beta^2}{cM^4}\right)^{1/3}\left(\frac{D_1}{\gamma^3}\right)^{1/6}\lambda^{2/3} \tag{24}$$

Thus, to obtain flutter boundaries a solution for the eigenvalue ψ as a function of the aerodynamic loading parameter λ was programed for a digital computer and utilized an eigenvalue routine for a square complex matrix. To obtain points of the flutter boundary for a particular panel, it is necessary to specify the panel geometric, stiffness, midplane loading, and structural damping characteristics as well as the degree of elastic rotational restraint present at the panel boundaries. The aerodynamic loading parameter λ is then varied until both equations (23) and (24) yield identical values of g_A. Limitations of the computer program restricted the maximum number of streamwise terms in the assumed deflection (eq. (14)) to 24. Hence, the program yields accurate results only for problems in which 24 terms are sufficient for convergence.

RESULTS AND DISCUSSION

Data are presented to evaluate the accuracy of the effects of aerodynamic damping given herein by the two-dimensional quasi-steady approximate aerodynamic theory as compared with the effects given in reference 5 by the more exact three-dimensional unsteady aerodynamic theory, to establish the validity of associating linear hysteretic structural damping with panel bending only, and to determine whether such a procedure yields a better correlation between theoretical and experimental panel flutter results. Although the analysis was developed in a general form to include orthotropic panels, results are presented for isotropic panels only. Comparison of representative results from the present analysis with results obtained from the exact analysis presented in reference 1 revealed that the present results were accurate for clamped panels having a length-width ratio less than about 8.

Damping Obtained From Aerodynamic Theories

Flutter results for a simply supported panel obtained from both two-dimensional quasi-steady aerodynamic theory and three-dimensional linearized supersonic potential flow theory presented in reference 14 and utilized in reference 5 are given in figure 2 for a panel with a length-width ratio of 4. The flutter parameter $\lambda^{1/3}$ is shown as a function of $k_x/k_{x,cr}$, the ratio of the midplane compressive load to the critical value required for buckling with no airflow. The dash-line curve represents the flutter boundary obtained from two-dimensional static aerodynamic theory (no damping). The numbers on this curve indicate the modes that coalesced for flutter. The circles represent flutter results from the three-dimensional potential flow theory taken from figure 9 of reference 5, which were

calculated from a six mode solution for aluminum panels at sea level for $M = 3.0$; this value of Mach number corresponds to the value at which most published experimental data for stressed panels have been obtained. The solid-line curve represents results from two-dimensional aerodynamic theory and was obtained by utilizing 10 modes in the present analysis. Structural damping was zero for all cases and for the present analysis aerodynamic damping is given by equation (24). The fact that the buckling load in the presence of airflow can be larger than that for no airflow causes the curves to extend beyond $\frac{k_x}{k_{x,cr}} = 1.0$. The buckling point on the flutter boundary in the presence of airflow is defined as the transition point. For no damping, the boundary indicates that zero values of the flutter parameter occur at values of $k_x/k_{x,cr}$ of approximately 0.58, 0.71, and 0.89. When the aerodynamic damping g_A is included in the calculations, the effect is the removal of the zero-dynamic-pressure points although the saw-toothed-like character of the boundary remains. As can be seen, the differences between the results from the two-dimensional quasi-steady aerodynamic theory and the three-dimensional potential flow theory are slight and may be considered insignificant in view of the fact that the latter results were obtained by a method which entailed a great deal of cross plotting of results from a six mode solution, which were probably not as well converged as the present results. Reference 5 shows that results from static aerodynamic theory agree reasonably well with those from three-dimensional potential flow theory for Mach numbers greater than 1.6; therefore, it is assumed that results from two-dimensional quasi-steady aerodynamic theory will also agree for $M > 1.6$. Two-dimensional quasi-steady aerodynamic theory does yield satisfactory results, when compared with results from three-dimensional potential flow theory, and provides a greatly simplified solution for many aeroelastic problems in which the effects of aerodynamic damping are important.

Effects of Structural Damping

Figure 3 illustrates the effects of structural damping on the flutter boundary presented in figure 2. The curves represent results from the present analysis for values of the aerodynamic damping coefficient from equation (24) for aluminum-alloy panels at sea level for $M = 3.0$. The dot-dash-line curve for no structural damping is taken from figure 2. The dash-line curve was obtained for a value of the bending and membrane structural damping coefficients equal to 0.01. The solid-line curve represents results for a value of the bending damping coefficient of 0.01 and a value of the membrane damping coefficient of zero. As shown by the dash-line curve, structural damping with equal bending and membrane damping coefficients tends to smooth out the saw-toothed-like flutter boundary; however, this effect lessens as $k_x/k_{x,cr}$ approaches the transition point. Similar results were obtained in reference 5 which used equal structural damping coefficients. Thus, this type of structural damping appears to have little effect on the

flutter of panels stressed to the point of buckling (transition point). However, as shown by the solid-line curve, when membrane damping is taken to be zero, structural damping smooths out the boundary to a greater degree and also raises the boundary at the point of buckling.

Since the effects of aerodynamic damping and structural damping with $g_B = g_M$ appear to be small as $k_x/k_{x,cr}$ approaches the transition point (see fig. 3), it is of interest to examine a special case for which the theory, damping neglected, predicts flutter at zero dynamic pressure at the panel buckling load. Such a condition is shown in figure 4 wherein the flutter parameter $\lambda^{1/3}$ is plotted as a function of $k_x/k_{x,cr}$ for a rotationally restrained panel with a length-width ratio of 3.3 and a stress ratio of $\frac{N_y}{N_x} = 1$. For this condition $k_{x,cr}$ is equivalent to $k_{x,T}$, the transition-point value of k_x. The lower solid-line curve represents the flutter boundary for no damping, and the dash-line curve represents the flutter boundary for $g_B = g_M = 0.01$ and values of g_A obtained from equation (24) for an assumed aluminum-alloy panel at Mach 3 and sea-level flow conditions. The upper solid-line curve is the flutter boundary obtained for the same flow conditions but with $g_M = 0$. As was shown in figure 3, if $g_B = g_M$, neither structural damping nor aerodynamic damping has any effect at the transition point (buckling point). Thus, for this special case (dash-line curve), theory predicts the occurrence of flutter at the transition point for zero dynamic pressure. This anomaly completely disappears when structural damping is associated with bending only. The trend of the flutter boundary thus obtained is physically reasonable and is typical of existing experimental boundaries. Therefore, it appears that structural damping is more realistically represented by modifying only the bending terms of the differential equation through use of complex stiffness coefficients.

Effects of Edge Rotational Restraint, Stress Ratio, and Length-Width Ratio on Transition Point Flutter

The structural damping results are particularly significant when it is realized that existing experimental results indicate that the most critical flutter condition occurs near or at the buckling point of the panel. This condition as defined by experiment is the transition point (intersection of prebuckled panel boundary and postbuckled panel boundary) and, as indicated in figure 4, past attempts at predicting the minimum value have in many instances led to the physically unreasonable zero values of dynamic pressure. Additionally, theoretical results which neglect damping or include structural damping in the form $g_B = g_M$ indicate that the transition point $\left(k_{x,cr} = k_{x,T}\right)$ is extremely sensitive to variations in edge rotational restraint, stress ratio, and length-width ratio. Therefore, results using the present representation of structural damping are presented concerning the effect of these parameters on transition point flutter.

Figure 5 illustrates the effect of varying edge rotational restraint for a panel having a length-width ratio of 3.3, a stress ratio of 1, and equal rotational springs on all edges. The flutter parameter at the transition point $\lambda_T^{1/3}$ is plotted as a function of the edge rotational restraint coefficient q_x. The lower curve represents results for any value of aerodynamic damping and any equal values of bending and membrane structural damping since damping included in this manner has no effect on flutter. The upper curve represents results for any value of aerodynamic damping and a value of bending structural damping of 0.01. A decrease in flutter resistance with an increase in restraint is exhibited by both curves. (This result agrees with ref. 1 wherein it was found that, for no damping, as edge rotational restraint increases, a stressed panel can become more susceptible to flutter even though its resistance to buckling increases.) In fact, the lower curve in figure 5 exhibits, at a value of $q_x = 40$, a zero-dynamic-pressure transition point. Not only does the present analysis eliminate this anomaly, as shown by the upper curve, it also predicts a less severe decrease in flutter margin with an increase in edge rotational restraint.

The effects of varying stress ratio on transition point flutter are illustrated in figure 6 for a panel having a length-width ratio of 4 and clamped edges. Again, the lower curve represents results which are unaffected by aerodynamic damping and structural damping when $g_B = g_M$, and the upper curve represents results obtained by associating structural damping with bending only. Comparison of the two curves reveals that associating structural damping with bending only not only removes the many zero-dynamic-pressure flutter points (which occur when the panel has an equal choice of buckling modes) but also gives a nearly constant value of the transition point flutter parameter over a wide range of stress ratio.

Figure 7 illustrates the effects of varying length-width ratio on the transition point flutter for a panel with clamped edges and a stress ratio N_y/N_x of 1. The lower curve represents results unaffected by damping, and the upper curve is again representative of results associated with bending structural damping only. Comparison of the two curves reveals that associating structural damping with bending only removes the extreme sensitivity of the transition point to variations in length-width ratio.

The results of figures 5, 6, and 7 suggest that the apparent sensitivity of critical flutter boundaries to edge rotational restraint, stress ratio, and length-width ratio was spurious and was associated largely with the anomalous zero values of critical dynamic pressure which, in turn, were due to an unrealistic theoretical model of structural damping.

Comparison of Theory and Experiment

The experimental flutter boundary presented in reference 2 for a panel with a length-width ratio of 2.9 and an average edge rotational restraint coefficient q_x of 44 is compared with theoretical boundaries obtained from the present analysis in figure 8. Only the portion corresponding to stresses below buckling is shown. Beyond buckling, the experimental boundary rises and small deflection theory is not sufficient to handle this condition. The boundaries are presented in terms of the flutter parameter $\lambda^{1/3}$ and the percent of midplane compressive load required for buckling in the presence of airflow. Theoretical boundaries are represented by the solid-line curves; the lower curve is for zero damping and the upper curve is based on an estimated bending damping coefficient g_B of 0.01 and values of the aerodynamic damping coefficient g_A calculated from the experimental test conditions. Reference 22 indicates that the maximum value of material damping for an aluminum alloy similar to that used in reference 2 is approximately 0.003. References 23 and 24 reveal that damping mechanisms present at panel boundaries may increase the structural damping up to five times the value for material damping. It is, therefore, believed that the estimated value of the bending damping coefficient of 0.01 is a realistic value for the experimental data represented by the circular symbols.

Agreement between the experimental boundary and the theoretical boundary for no damping is reasonably good for low values of midplane compressive stress but becomes poor in the region of the transition point. Aerodynamic damping and structural damping associated with bending only improves the agreement at the transition point, but the theory remains conservative. The values of q_x for the points shown range from about 27 to ∞ or fully clamped. Therefore, it is believed that the experimental boundary is not truly representative of a boundary for $q_x = 44$ and that some scatter should be expected. Thus, a need exists for experimental flutter boundaries wherein the variation of q_x is not so large to provide data for a more adequate evaluation of the present theory.

CONCLUSIONS

The flutter of stressed panels with elastic edge rotational restraint was investigated theoretically. A modal solution which includes both structural and aerodynamic damping was presented for the supersonic flutter of flat orthotropic panels. The solution utilizes two-dimensional quasi-steady aerodynamics and is valid for panels with nondeflecting edges. The theoretical results and the comparison of a theoretical boundary from the present analysis with an experimental boundary presented in NASA TN D-3498 revealed that the following conclusions can be made:

1. Two-dimensional quasi-steady aerodynamic theory yields satisfactory results when compared with three-dimensional potential flow theory for $M > 1.6$ and may provide greatly simplified solutions to aeroelastic problems wherein the effects of aerodynamic damping are important.

2. Inclusion of structural damping in a small deflection plate theory is more realistically accomplished by modifying only the bending terms of the differential equation through the use of complex bending stiffness coefficients; such a representation removes all physically untenable results that otherwise occur and provides reasonable agreement between theoretical and experimental panel flutter results over the entire stress range from zero to buckling.

3. Representation of structural damping by use of complex bending stiffness coefficients renders the flutter parameter at the transition point (transition from flat to buckled panel) relatively insensitive to variations in edge rotational restraint, stress ratio, and length-width ratio.

The ability to predict experimental results with reasonable accuracy over the entire stress range makes it possible to consider the flutter design of stressed panels on a rational analytical basis rather than continuing to rely on empirical boundaries which must be periodically revised as new experimental data are obtained.

Langley Research Center,
National Aeronautics and Space Administration,
Langley Station, Hampton, Va., September 23, 1968,
126-14-02-22-23.

APPENDIX

SOLUTION TO FLUTTER EQUATION

A solution to the flutter equation (eq. (8)) may be obtained by application of the Galerkin technique. Substitution of the assumed deflection given by equation (14) into equation (8), multiplying by $F_m\left(\frac{x}{a}\right)G_1\left(\frac{y}{b}\right)$, and integrating over the area results in the following set of equations for the amplitude coefficients A_{r1}:

$$\sum_{r=1}^{k}\left\{\left(1+ig_B\right)\left[\frac{(I_1)_{mr}}{\pi^4}+2\left(\frac{a}{b}\right)^2\frac{D_{12}}{D_1}\frac{C_1}{\pi^4 C_0}(I_2)_{mr}+\left(\frac{a}{b}\right)^4\frac{D_2}{D_1}\frac{C_2}{\pi^4 C_0}(I_3)_{mr}\right]\right.$$

$$+\left(1+ig_M\right)\left[\frac{k_x}{\pi^2}\left(\frac{a}{b}\right)^2(I_2)_{mr}+k_y\left(\frac{a}{b}\right)^4\frac{C_1}{\pi^2 C_0}(I_3)_{mr}\right]$$

$$\left.+\left(\frac{\alpha^2}{\omega_r^2}+g_A\frac{\alpha}{\omega_r}\right)(I_3)_{mr}+\frac{\lambda}{\pi^4}L_{mr}\right\}A_{r1}=0 \qquad (m=1,2,3,\ldots,k) \quad \text{(A1)}$$

where

$$\left.\begin{aligned} C_0&=\int_{-1/2}^{1/2}G_1^2\left(\frac{y}{b}\right)d\left(\frac{y}{b}\right)\\ C_1&=\int_{-1/2}^{1/2}G_1\left(\frac{y}{b}\right)G_1''\left(\frac{y}{b}\right)d\left(\frac{y}{b}\right)\\ C_2&=\int_{-1/2}^{1/2}G_1\left(\frac{y}{b}\right)G_1^{IV}\left(\frac{y}{b}\right)d\left(\frac{y}{b}\right)\end{aligned}\right\} \quad \text{(A2)}$$

and

$$(I_1)_{mr}=\int_{-1/2}^{1/2}F_m\left(\frac{x}{a}\right)F_r^{IV}\left(\frac{x}{a}\right)d\left(\frac{x}{a}\right)=\begin{cases}(J_1)_{mm} & \text{for } m=r \text{ if } m \text{ and } r \text{ odd}\\ (K_1)_{mm} & \text{for } m=r \text{ if } m \text{ and } r \text{ even}\\ 0 & \text{for } m\neq r\end{cases} \quad \text{(A3)}$$

APPENDIX

$$(I_2)_{mr} = \int_{-1/2}^{1/2} F_m\left(\frac{x}{a}\right) F_r''\left(\frac{x}{a}\right) d\left(\frac{x}{a}\right) = \begin{cases} (J_2)_{mm} & \text{for } m = r \text{ if } m \text{ and } r \text{ odd} \\ (J_2)_{mr} & \text{for } m \neq r \text{ if } m \text{ and } r \text{ odd} \\ (K_2)_{mm} & \text{for } m = r \text{ if } m \text{ and } r \text{ even} \\ (K_2)_{mr} & \text{for } m \neq r \text{ if } m \text{ and } r \text{ even} \end{cases} \tag{A4}$$

$$(I_3)_{mr} = \int_{-1/2}^{1/2} F_m\left(\frac{x}{a}\right) F_r\left(\frac{x}{a}\right) d\left(\frac{x}{a}\right) = \begin{cases} (J_3)_{mm} & \text{for } m = r \text{ if } m \text{ and } r \text{ odd} \\ (K_3)_{mm} & \text{for } m = r \text{ if } m \text{ and } r \text{ even} \\ 0 & \text{for } m \neq r \end{cases} \tag{A5}$$

$$L_{mr} = \int_{-1/2}^{1/2} F_m\left(\frac{x}{a}\right) F_r'\left(\frac{x}{a}\right) d\left(\frac{x}{a}\right) = \begin{cases} 0 & \text{for } m + r = \text{Even} \\ \bar{L}_{mr} & \text{for } m \text{ odd} \\ \hat{L}_{mr} & \text{for } m \text{ even} \end{cases} \tag{A6}$$

The primes and superscript Roman numeral denote differentiation with respect to $\frac{x}{a}$ or $\frac{y}{b}$.

The integrals in equations (A3) to (A6) are evaluated in terms of the expressions on the right-hand sides of these equations by use of the following deflection functions for the zero stress vibrations of beams with equal end rotational restraint (see ref. 25):

Symmetrical modes

$$F_j\left(\frac{x}{a}\right) = \cos 2\delta_j \frac{x}{a} - \frac{\cos \delta_j}{\cosh \delta_j} \cosh 2\delta_j \frac{x}{a} \qquad (j = 1, 3, 5 \ldots) \tag{A7}$$

Asymmetrical modes

$$F_j\left(\frac{x}{a}\right) = \sin 2\delta_j \frac{x}{a} - \frac{\sin \delta_j}{\sinh \delta_j} \sinh 2\delta_j \frac{x}{a} \qquad (j = 2, 4, 6 \ldots) \tag{A8}$$

where δ_j is a constant dependent on the degree of rotational restraint. The expressions for determining δ_j from reference 25 in the terminology of the present analysis are as follows:

APPENDIX

Symmetrical modes

$$\frac{\delta_j}{q_x} = -\frac{1}{4}\left(\tan \delta_j + \tanh \delta_j\right) \tag{A9}$$

Asymmetrical modes

$$\frac{\delta_j}{q_x} = \frac{1}{4}\left(\cot \delta_j - \coth \delta_j\right) \tag{A10}$$

where

$$q_x = \frac{a\theta_x}{D_1} \tag{A11}$$

The integral expressions in equations (A2) may be evaluated by use of equations (A7) to (A9), that is, replacing $\frac{x}{a}$ with $\frac{y}{b}$, replacing q_x with $q_y = \frac{b\theta_y}{D_2}$, and taking $j = 1$. Expressions for the integrals in equations (A3) to (A6) are given as follows:

$$\left(J_1\right)_{mm} = 8\delta_m{}^4\left(1 + \frac{\cos^2\delta_m}{\cosh^2\delta_m} - \frac{\cos \delta_m \sin \delta_m}{\delta_m} - \frac{\cos^2\delta_m}{\delta_m}\tanh \delta_m\right) \tag{A12}$$

$$\left(J_2\right)_{mm} = 2\delta_m{}^2\left(\frac{\cos^2\delta_m}{\cosh^2\delta_m} - 1\right) + 2\delta_m \cos \delta_m\left(\cos \delta_m \tanh \delta_m - \sin \delta_m\right) \tag{A13}$$

$$\left(J_2\right)_{mr} = \frac{8\delta_m{}^2\delta_r{}^2}{\delta_r{}^4 - \delta_m{}^4}\Big[\delta_m \sin \delta_m \cos \delta_r - \delta_r \cos \delta_m \sin \delta_r$$

$$- \cos \delta_r \cos \delta_m\left(\delta_m \tanh \delta_m - \delta_r \tanh \delta_r\right)\Big] \tag{A14}$$

$$\left(J_3\right)_{mm} = \frac{1}{2}\left(1 + \frac{\cos^2\delta_m}{\cosh^2\delta_m} - \frac{\cos \delta_m \sin \delta_m}{\delta_m} - \frac{\cos^2\delta_m}{\delta_m}\tanh \delta_m\right) \tag{A15}$$

$$\left(K_1\right)_{mm} = 8\delta_m{}^4\left(1 - \frac{\sin^2\delta_m}{\sinh^2\delta_m} + \frac{\sin \delta_m \cos \delta_m}{\delta_m} - \frac{\sin^2\delta_m}{\delta_m}\coth \delta_m\right) \tag{A16}$$

$$\left(K_2\right)_{mm} = -2\delta_m{}^2\left(\frac{\sin^2\delta_m}{\sinh^2\delta_m} + 1\right) + 2\delta_m \sin \delta_m\left(\sin \delta_m \coth \delta_m + \cos \delta_m\right) \tag{A17}$$

APPENDIX

$$(K_2)_{mr} = -\frac{8\delta_m^2\delta_r^2}{\delta_r^4 - \delta_m^4}\Big[\delta_m \cos\delta_m \sin\delta_r - \delta_r \cos\delta_r \sin\delta_m$$

$$+ \sin\delta_m \sin\delta_r(\delta_m \coth\delta_m - \delta_r \coth\delta_r)\Big] \tag{A18}$$

$$(K_3)_{mm} = \frac{1}{2}\left(1 - \frac{\sin^2\delta_m}{\sinh^2\delta_m} + \frac{\sin\delta_m \cos\delta_m}{\delta_m} - \frac{\sin^2\delta_m}{\delta_m}\coth\delta_m\right) \tag{A19}$$

$$\bar{L}_{mr} = \frac{8\delta_r^2\delta_m^2}{\delta_r^4 - \delta_m^4}\sin\delta_r \cos\delta_m - 2\delta_m\delta_r\left[\frac{\cos\delta_r \cos\delta_m \tanh\delta_m + \sin\delta_r \sin\delta_m \coth\delta_r}{\delta_m^2 + \delta_r^2}\right.$$

$$\left. + \left(\frac{\cos\delta_r \sin\delta_m + \sin\delta_r \cos\delta_m \coth\delta_r \tanh\delta_m}{\delta_r^2 - \delta_m^2}\right)\right] \tag{A20}$$

$$\hat{L}_{mr} = \frac{8\delta_r^2\delta_m^2}{\delta_r^4 - \delta_m^4}\cos\delta_r \sin\delta_m + 2\delta_m\delta_r\left[\frac{\cos\delta_r \cos\delta_m \tanh\delta_r + \sin\delta_r \sin\delta_m \coth\delta_m}{\delta_m^2 + \delta_r^2}\right.$$

$$\left. - \left(\frac{\sin\delta_r \cos\delta_m + \cos\delta_r \sin\delta_m \tanh\delta_r \coth\delta_m}{\delta_r^2 - \delta_m^2}\right)\right] \tag{A21}$$

For a nontrivial solution to equation (A1) the determinant of the coefficients of A_{r1} must be zero. The determinant is given in the main text (eq. (16)).

REFERENCES

1. Erickson, Larry L.: Supersonic Flutter of Flat Rectangular Orthotropic Panels Elastically Restrained Against Edge Rotation. NASA TN D-3500, 1966.

2. Shideler, John L.; Dixon, Sidney C.; and Shore, Charles P.: Flutter at Mach 3 of Thermally Stressed Panels and Comparison With Theory for Panels With Edge Rotational Restraint. NASA TN D-3498, 1966.

3. Dixon, Sidney C.: Application of Transtability Concept to Flutter of Finite Panels and Experimental Results. NASA TN D-1948, 1963.

4. Guy, Lawrence D.; and Dixon, Sidney C.: A Critical Review of Experiment and Theory for Flutter of Aerodynamically Heated Panels. Symposium on Dynamics of Manned Lifting Planetary Entry, S. M. Scala, A. C. Harrison, and M. Rogers, eds., John Wiley & Sons, Inc., c.1963, pp. 568-595.

5. Dixon, Sidney C.: Comparison of Panel Flutter Results From Approximate Aerodynamic Theory With Results From Exact Inviscid Theory and Experiment. NASA TN D-3649, 1966.

6. Dowell, Earl: Flutter of Multibay Panels at High Supersonic Speeds. AIAA J., vol. 2, no. 10, Oct. 1964, pp. 1805-1814.

7. Dugundji, John: Theoretical Considerations of Panel Flutter at High Supersonic Mach Numbers. AIAA J., vol. 4, no. 7, July 1966, pp. 1257-1266.

8. Lazan, B. J.: Energy Dissipation Mechanisms In Structures, With Particular Reference to Material Damping. Structural Damping, Jerome E. Ruzicka, ed., Amer. Soc. Mech. Eng., c.1959, pp. 1-34.

9. Lazan, B. J.: Damping Studies in Materials Science and Materials Engineering. Internal Friction, Damping, and Cyclic Plasticity, Spec. Tech. Publ. No. 378, Amer. Soc. Testing Mater., c.1965, pp. 1-20.

10. Nelson, Herbert C.; and Cunningham, Herbert J.: Theoretical Investigation of Flutter of Two-Dimensional Flat Panels With One Surface Exposed to Supersonic Potential Flow. NACA Rep. 1280, 1956. (Supersedes NACA TN 3465.)

11. Dowell, E. H.; and Voss, H. M.: Theoretical and Experimental Panel Flutter Studies in the Mach Number Range 1.0 to 5.0. AIAA J., vol. 3, no. 12, Dec. 1965, pp. 2292-2304.

12. Johns, D. J.; and Parks, P. C.: Effect of Structural Damping on Panel Flutter. Aircraft Eng., vol. XXXII, no. 380, Oct. 1960, pp. 304-308.

13. Kobett, D. R.; and Zeydel, E. F. E.: Research on Panel Flutter. NASA TN D-2227, 1963.

14. Cunningham, Herbert J.: Flutter Analysis of Flat Rectangular Panels Based on Three-Dimensional Supersonic Unsteady Potential Flow. NASA TR R-256, 1967.

15. Herrmann, George: The Influence of Initial Stress on the Dynamic Behaviour of Elastic and Viscoelastic Plates. Publ. Int. Ass. Bridge Struct. Eng., vol. 16, 1956, pp. 275-294.

16. Libove, Charles; and Batdorf, S. B.: A General Small-Deflection Theory for Flat Sandwich Plates. NACA Rep. 899, 1948. (Supersedes NACA TN 1526.)

17. Houbolt, John Cornelius: A Study of Several Aerothermoelastic Problems of Aircraft Structures in High-Speed Flight. Prom. Nr. 2760, Swiss Fed. Inst. Technol. (Zürich), 1958.

18. Hedgepeth, John M.: Flutter of Rectangular Simply Supported Panels at High Supersonic Speeds. J. Aeronaut. Sci., vol. 24, no. 8, Aug. 1957, pp. 563-573, 586.

19. Ketter, D. J.: Flutter of Flat, Rectangular, Orthotropic Panels. AIAA J., vol. 5, no. 1, Jan. 1967, pp. 116-124.

20. Fraeijs de Veubeke, B. M.: Influence of Internal Damping on Aircraft Resonance. Structural Aspects. Pt. I of AGARD Manual on Aeroelasticity, ch. 3, W. P. Jones, ed.

21. Scanlan, R. H.; and Mendelson, A.: Structural Damping. AIAA J. (Tech. Notes Comments), vol. 1, no. 4, Apr. 1963, pp. 938-939.

22. Granick, Neal; and Stern, Jesse E.: Material Damping of Aluminum by a Resonant-Dwell Technique. NASA TN D-2893, 1965.

23. Mentel, T. J.; and Schultz, R. L.: Viscoelastic Support Damping of Built-In Circular Plates. ASD-TDR-63-648, U.S. Air Force, Oct. 1963.

24. Ungar, Eric E.: Energy Dissipation at Structural Joints; Mechanisms and Magnitudes. FDL-TDR-64-98, U.S. Air Force, Aug. 1964.

25. Weeks, George E.; and Shideler, John L.: Effect of Edge Loadings on the Vibration of Rectangular Plates With Various Boundary Conditions. NASA TN D-2815, 1965.

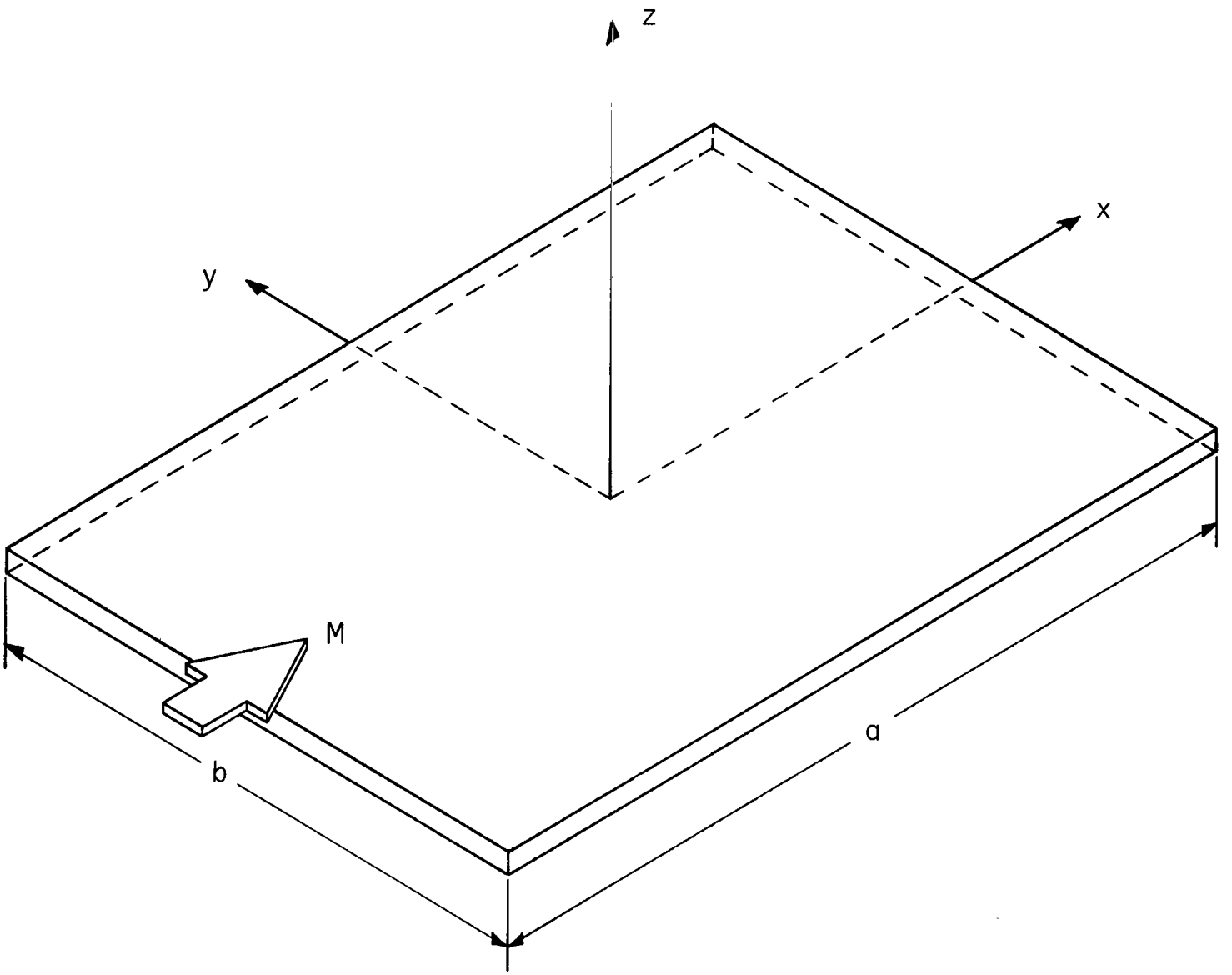

Figure 1.- Coordinate system of orthotropic panel and direction of airflow.

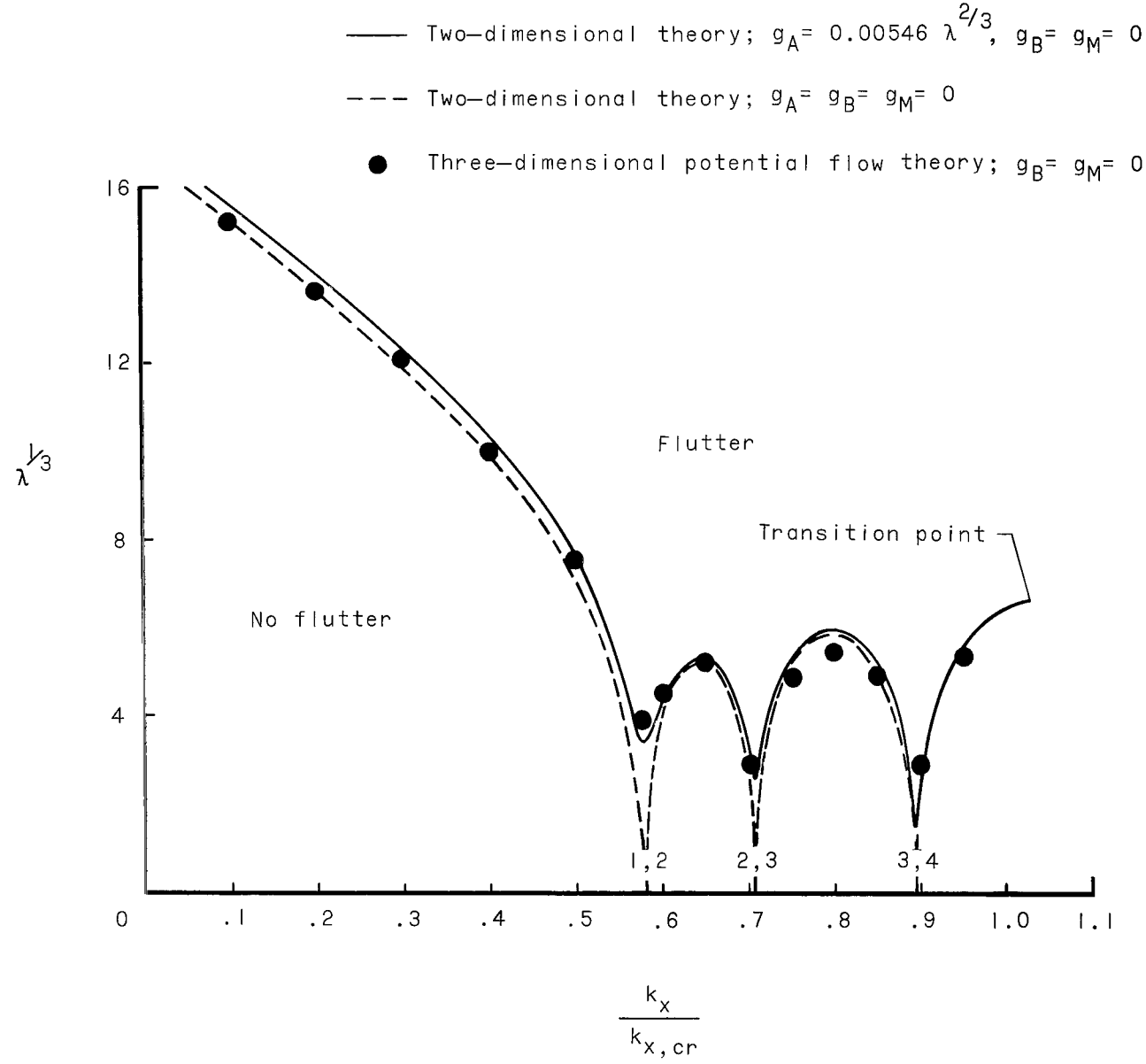

Figure 2.- Three-dimensional potential flow theory and two-dimensional quasi-steady aerodynamic theory for a flat simply supported aluminum-alloy panel subjected to midplane compressive load. $M = 3.0$; $\frac{a}{b} = 4.0$; $\frac{N_y}{N_x} = 0$. The numbers on the dash-line curve indicate the modes that coalesced for flutter.

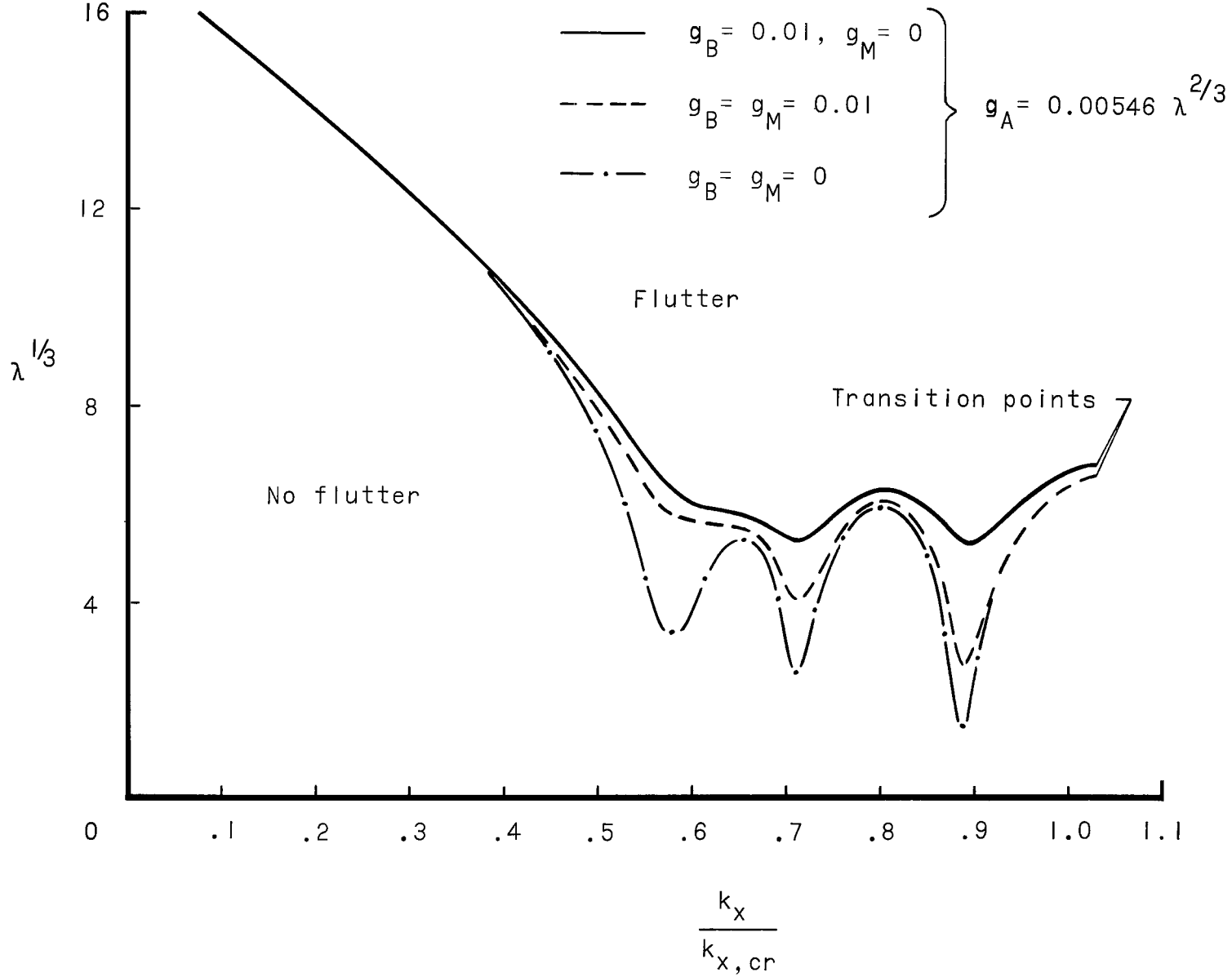

Figure 3.- Effects of structural damping on the flutter boundary for a simply supported aluminum-alloy panel at sea level. $M = 3.0$; $\frac{a}{b} = 4.0$; $\frac{N_y}{N_x} = 0$.

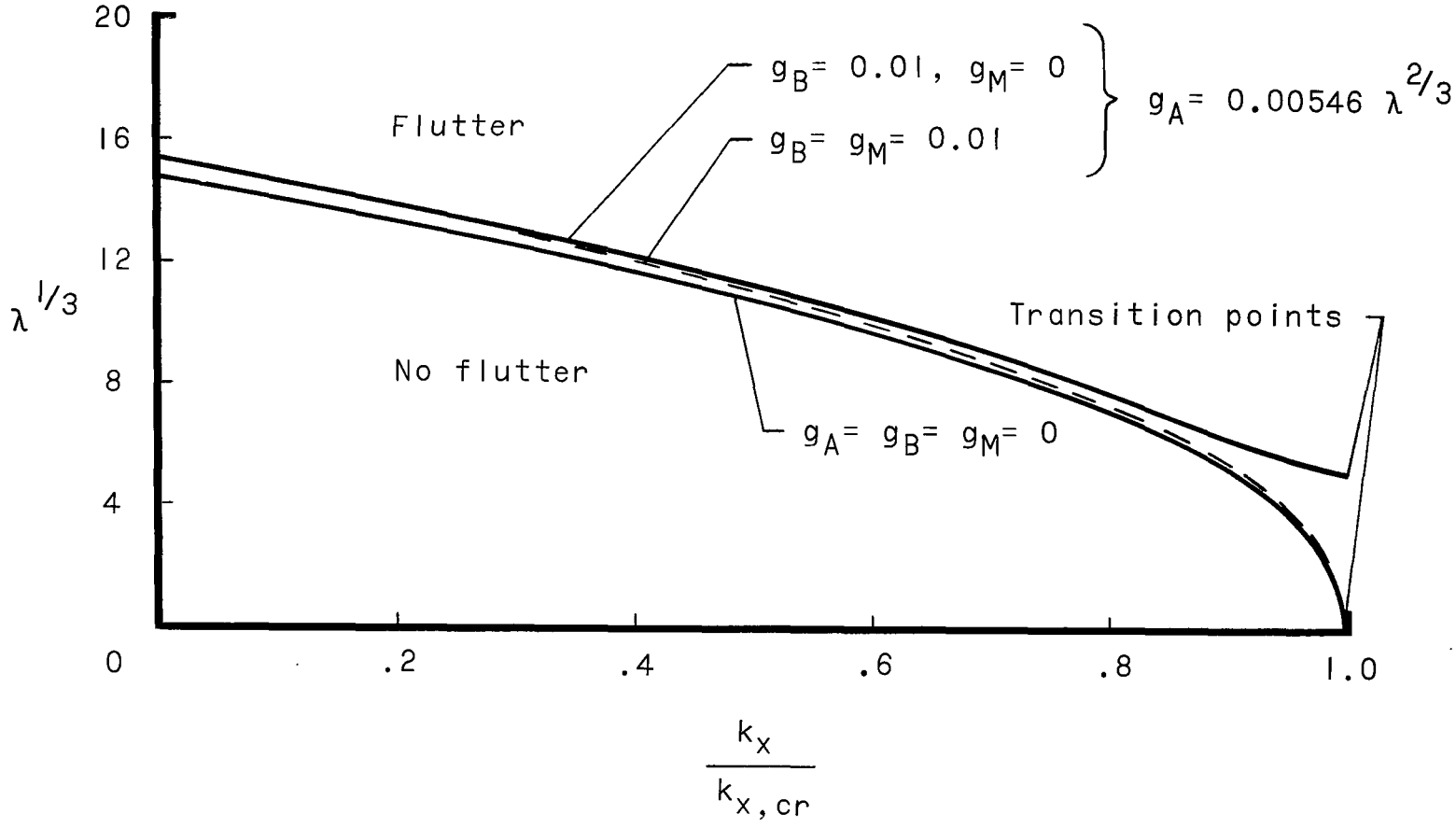

Figure 4.- Effects of structural and aerodynamic damping on flutter of a flat rotationally restrained panel subjected to midplane load. $\frac{a}{b} = 3.3$; $\frac{N_y}{N_x} = 1$; $\theta_x = \theta_y$; $q_x = 40$.

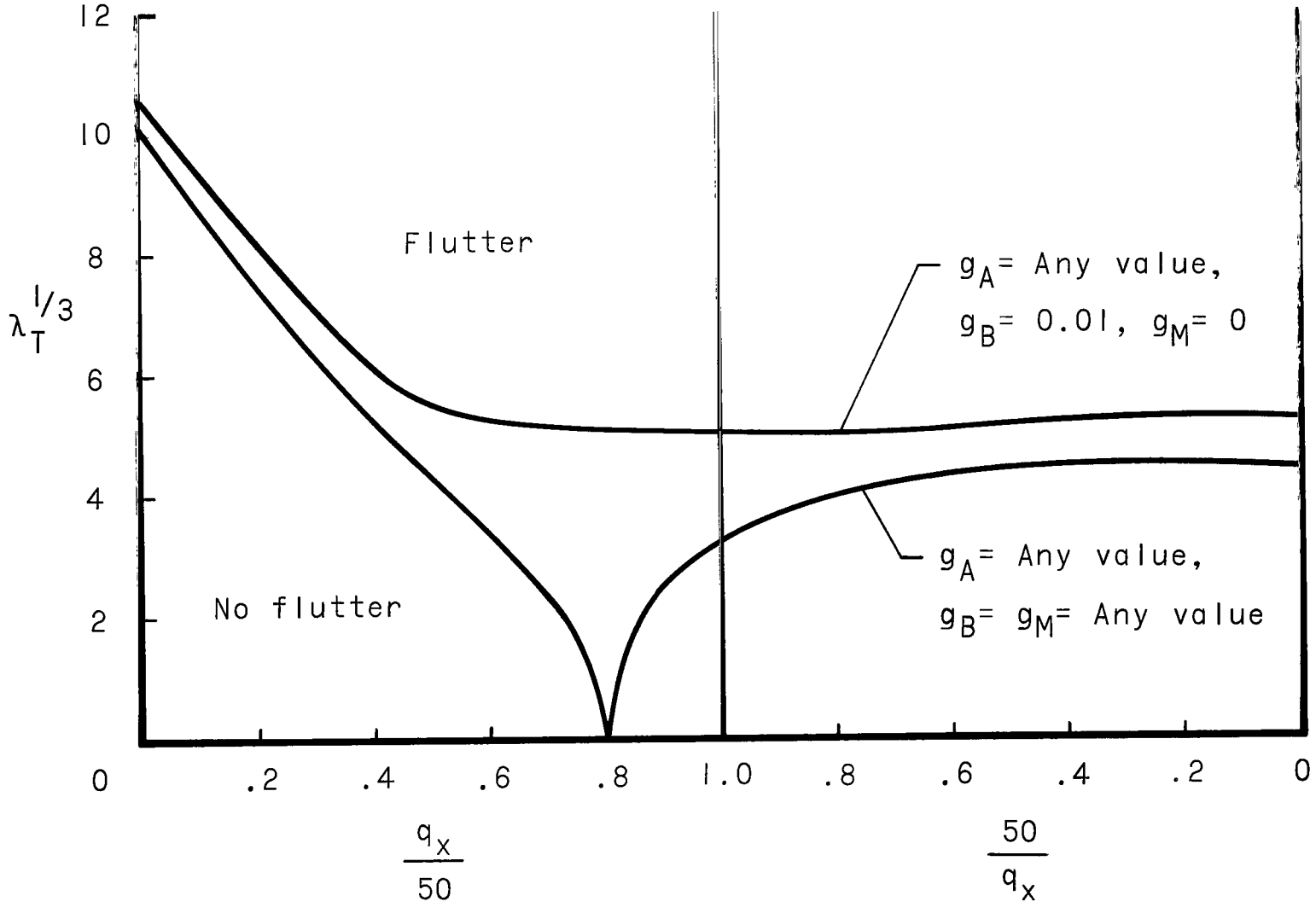

Figure 5.- Effects of edge rotational restraint and damping on transition point flutter. $\frac{a}{b} = 3.3$; $\frac{N_y}{N_x} = 1$; $\theta_x = \theta_y$.

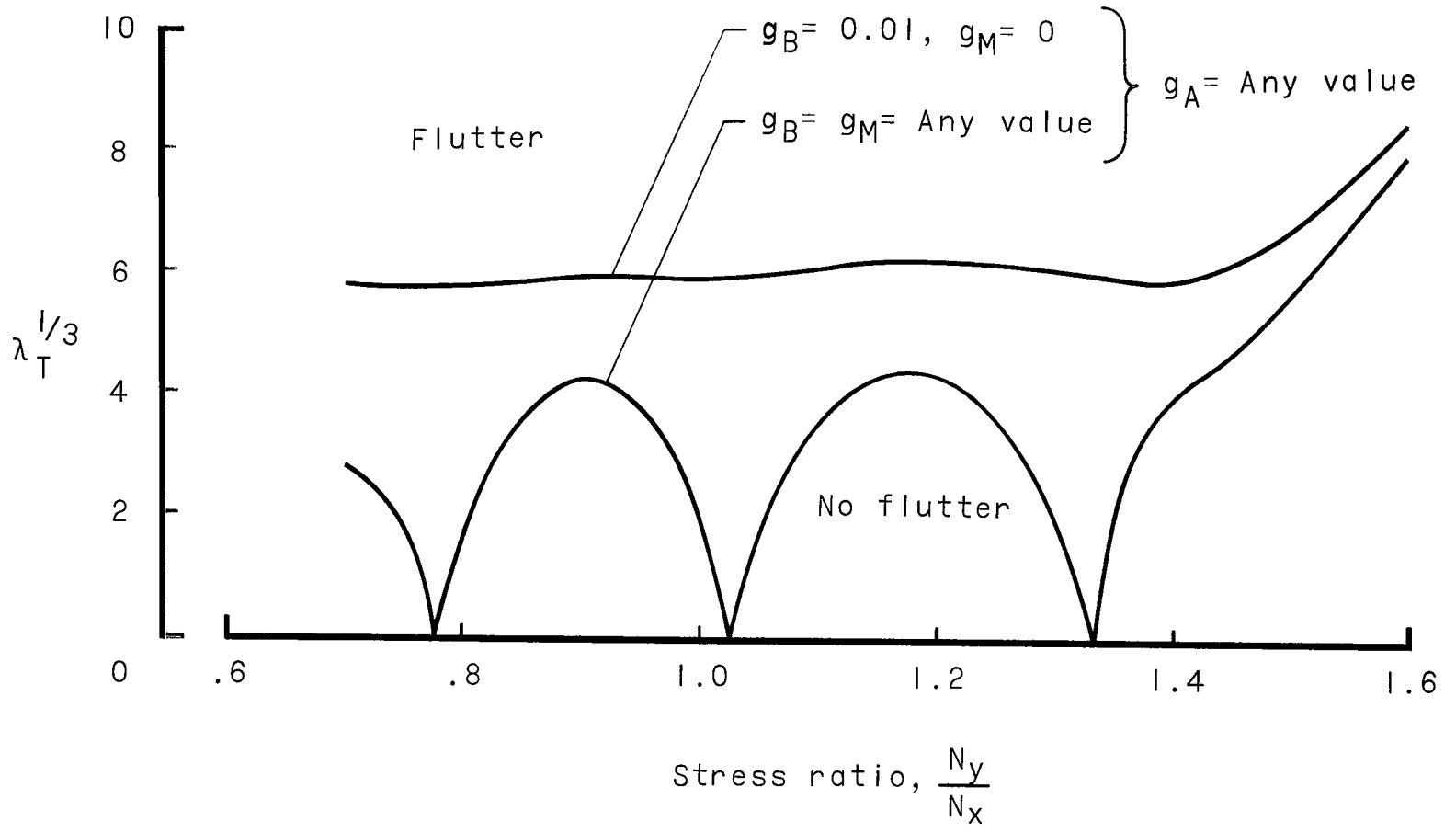

Figure 6.- Effects of stress ratio and damping on transition point flutter for a panel having $\frac{a}{b} = 4$ and clamped edges.

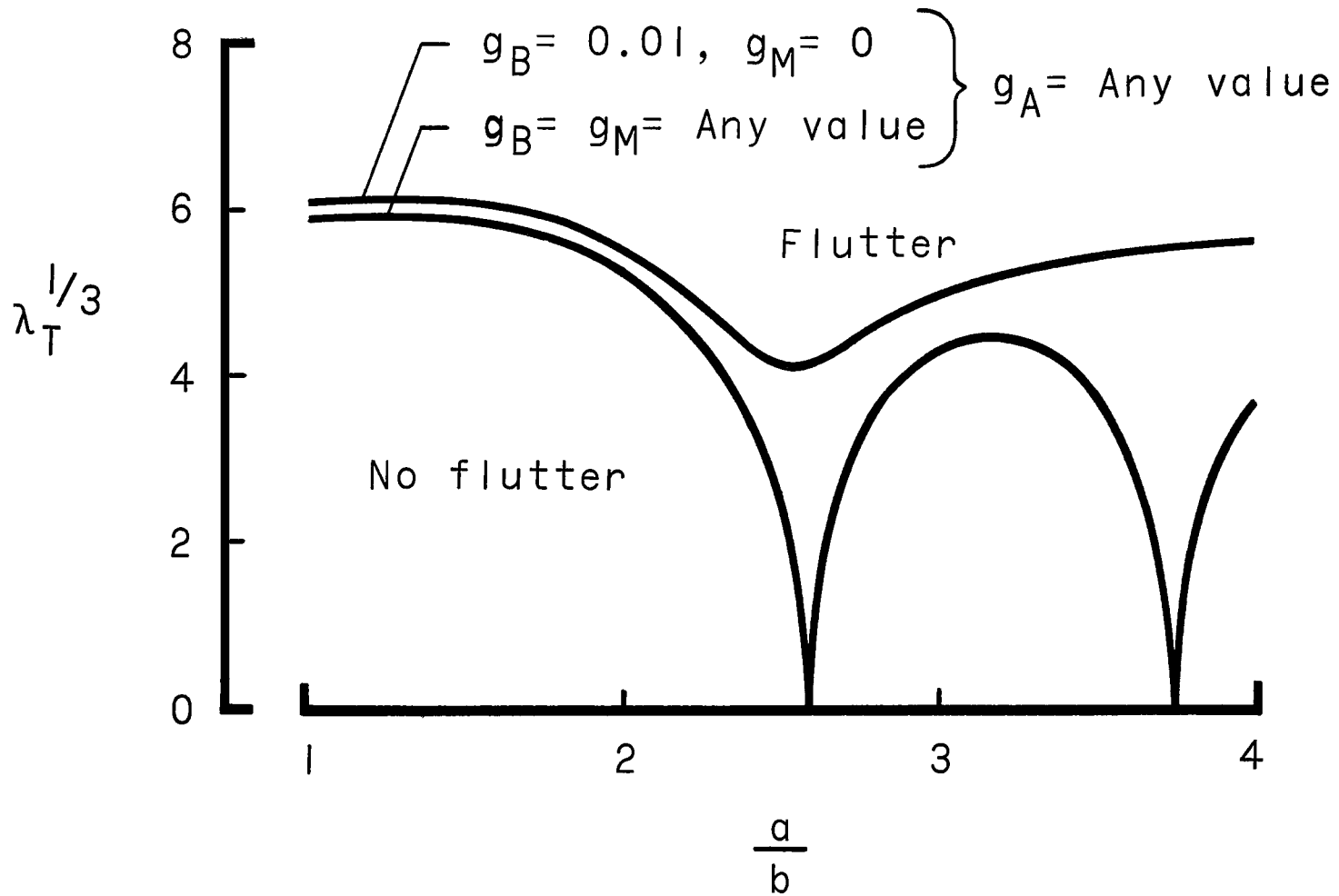

Figure 7.- Effects of length-width ratio and damping on transition point flutter for a panel with clamped edges and $\frac{N_y}{N_x} = 1$.

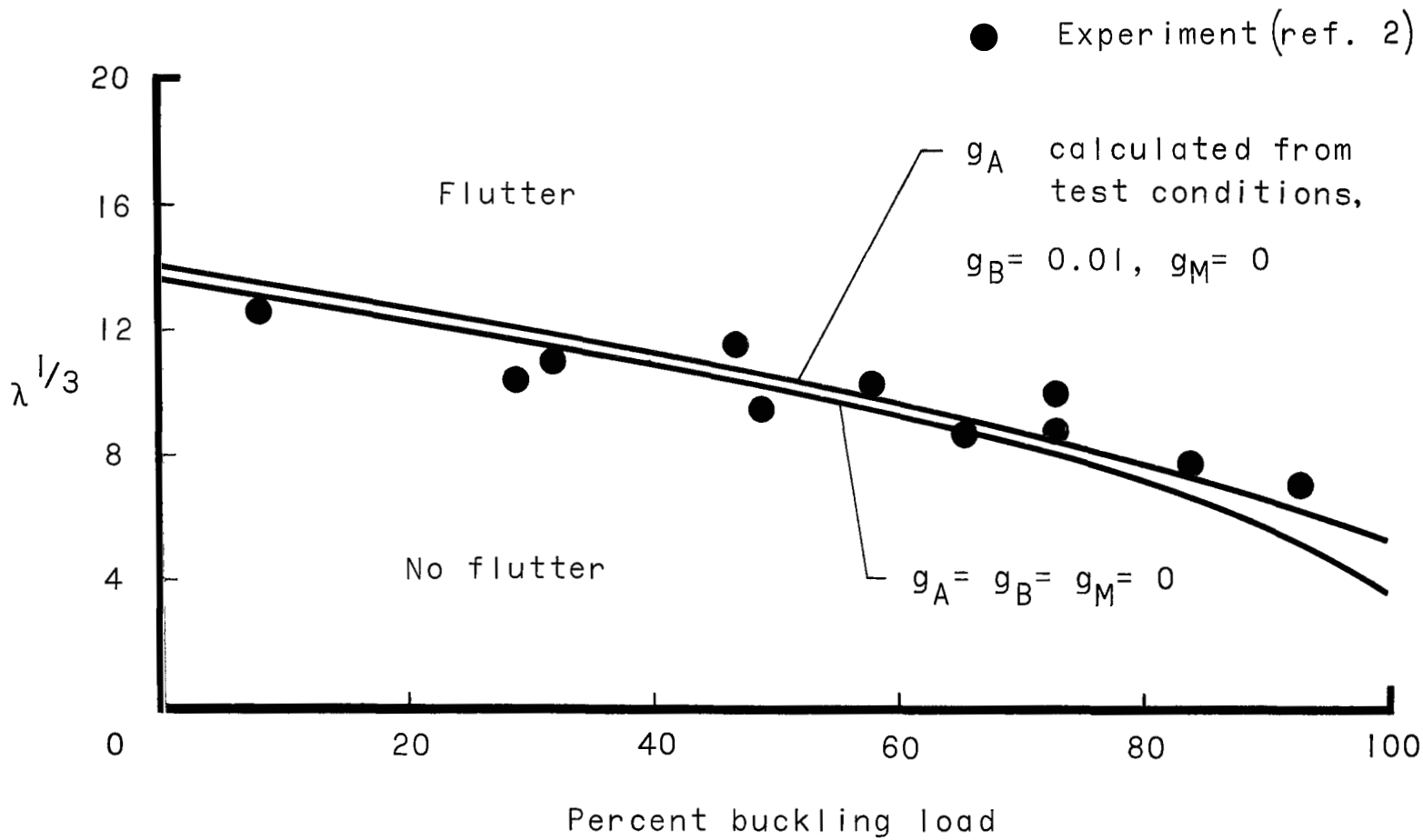

Figure 8.- Flat panel portion of experimental boundary of reference 2 and theoretical boundaries of present analysis. $\frac{a}{b} = 2.9$; $\frac{N_y}{N_x} = 1$; $\theta_x = \theta_y$; average value of q_x of 44.

NATIONAL AERONAUTICS AND SPACE ADMINISTRATION
WASHINGTON, D. C. 20546
OFFICIAL BUSINESS

FIRST CLASS MAIL

POSTAGE AND FEES PAID
NATIONAL AERONAUTICS AND
SPACE ADMINISTRATION

"The aeronautical and space activities of the United States shall be conducted so as to contribute . . . to the expansion of human knowledge of phenomena in the atmosphere and space. The Administration shall provide for the widest practicable and appropriate dissemination of information concerning its activities and the results thereof."

—NATIONAL AERONAUTICS AND SPACE ACT OF 1958

NASA SCIENTIFIC AND TECHNICAL PUBLICATIONS

TECHNICAL REPORTS: Scientific and technical information considered important, complete, and a lasting contribution to existing knowledge.

TECHNICAL NOTES: Information less broad in scope but nevertheless of importance as a contribution to existing knowledge.

TECHNICAL MEMORANDUMS: Information receiving limited distribution because of preliminary data, security classification, or other reasons.

CONTRACTOR REPORTS: Scientific and technical information generated under a NASA contract or grant and considered an important contribution to existing knowledge.

TECHNICAL TRANSLATIONS: Information published in a foreign language considered to merit NASA distribution in English.

SPECIAL PUBLICATIONS: Information derived from or of value to NASA activities. Publications include conference proceedings, monographs, data compilations, handbooks, sourcebooks, and special bibliographies.

TECHNOLOGY UTILIZATION PUBLICATIONS: Information on technology used by NASA that may be of particular interest in commercial and other non-aerospace applications. Publications include Tech Briefs, Technology Utilization Reports and Notes, and Technology Surveys.

Details on the availability of these publications may be obtained from:

SCIENTIFIC AND TECHNICAL INFORMATION DIVISION

NATIONAL AERONAUTICS AND SPACE ADMINISTRATION

Washington, D.C. 20546